

MESON CLOUD EFFECTS IN NUCLEON RESONANCES AT LOW AND INTERMEDIATE ENERGIES*

BOJAN GOLLI

Faculty of Education, University of Ljubljana, 1000 Ljubljana, Slovenia
and
Jožef Stefan Institute, 1000 Ljubljana, Slovenia

(Received December 5, 2014)

We review some results obtained by the Coimbra–Ljubljana collaboration that reveal the important role of the pion cloud in the low- and intermediate-energy nucleon and delta resonances.

DOI:10.5506/APhysPolBSupp.8.213

PACS numbers: 25.80.Ek, 12.39.Fe, 13.60.Le, 14.20.Gk

1. Introduction

The notion that the pion cloud plays an important role in the formation of nucleon resonances was first anticipated by da Providência and Urbano in 1978 [1]. In their work, the nucleon resonances arise as excitations of the pion cloud around the bare nucleon. The classical pion field was interpreted as a coherent state of pions and the resonances with good angular momentum and isospin were obtained by Peierls–Yoccoz projection. This approach is similar to the so-called model of *dynamical generation* of resonances. On the other hand, in the *quark model*, the resonances emerge as excitations of the three-quark core. In early eighties, we started a long term collaboration between the Coimbra group (J. da Providência, M. Fiolhais, P. Alberto, and L. Amoreira) and the Ljubljana group (M. Rosina, S. Širca, M. Čibej and B.G.). In our work, we have combined both approaches assuming a superposition of different excitations of the quark core surrounded by meson clouds. In such a picture, some resonances can be described as almost pure single-quark excitations of the core, while for other resonances

* Talk presented at the EEF70 Workshop on Unquenched Hadron Spectroscopy: Non-Perturbative Models and Methods of QCD *vs.* Experiment, Coimbra, Portugal, September 1–5, 2014.

the main mechanism is the excitation of the meson cloud. How can we determine which mechanism dominates in a given resonance? If we investigate just meson scattering in the resonance region, we may not reliably determine the nature of the resonance since, by a suitable modification of the coupling constants and the interaction range, it is possible to reproduce reasonably well the elastic and inelastic amplitudes almost in any model. We claim that studying meson electro-production processes, in particular the Q^2 -dependence of helicity amplitudes, is a much more severe test to analyse the structure of various resonances.

In the next sections, we present some examples in which we have established the important role of the meson cloud. We have considered different chiral quark models, the linear σ -model with quarks, the chromodielectric model in which a dynamical confinement is generated by an additional scalar field, and the cloudy bag model, which turns out to be suitable for the description of higher resonances.

2. The $\Delta(1232)$ resonance

The $\Delta(1232)$ was the first resonance that we tackled. We assumed a superposition of the bare Δ core with three quarks in the $1s$ orbit with the spins and isospins coupled to $3/2$, and the pion cloud around the bare nucleon and the bare Δ core. Using Peierls–Yoccoz projection, we maintained the correct spin and isospin of the composite state. We calculated the electromagnetic transition amplitudes as a function of the photon virtuality Q^2 . We found that the processes in which the photon interacts with the pion cloud importantly contribute to the helicity amplitude [2]. For the leading magnetic dipole contribution (M1), we could have anticipated such a result from our experience with the nucleon magnetic moments. On the other hand, the quadrupole excitations, the transverse E2 and the Coulomb C2 are not allowed in the nucleon, but are present in the transition N to Δ amplitude. We have found relatively large quadrupole amplitudes originating from the p -wave pion flip of its third component of the angular momentum (see Fig. 1). In a quark model without pions such a strong contribution could only be possible if we assumed an unrealistically strong admixture of the d -wave quark configuration. To the best of our knowledge, we were the first to calculate the Q^2 behavior of the E2 and C2 amplitude. We showed that the different Q^2 behavior of these amplitudes (equal for a point-like source) originates from the long-range part of N and Δ wave function which is dominated by the pion tail. Since then, our result has been rediscovered in different approaches and supported by new, more precise measurements.

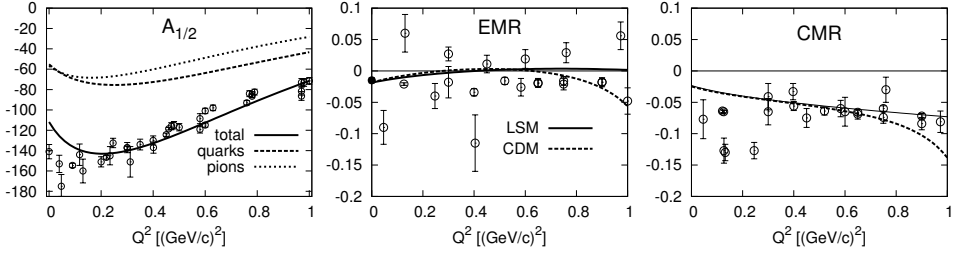


Fig. 1. The separate quark and pion contributions to the helicity amplitude $A_{1/2}$ in units of $10^{-3} \text{ GeV}^{-1/2}$ calculated in the linear σ -model (left panel), the ratio E2/M1 (middle panel) and C2/M1 (right panel) calculated in the linear σ -model and in the chromodielectric model.

3. The multi-channel approach

While for the $\Delta(1232)$ resonance the inelastic channels can be ignored, they have to be included if we want to study higher resonance. We have developed an approach for computing the multi-channel K matrix which includes many-body quasi-bound quark states in the scattering formalism [3]. In this approach, the channel state corresponding to the scattering baryon and meson is (up to the normalization factor) given by

$$|\Psi_{JI}^{MB}\rangle = a^\dagger(k)|\Psi_B\rangle + c_{\mathcal{R}}|\Phi_{\mathcal{R}}\rangle + \sum_{M'B'} \int \frac{dk' \chi^{M'B'MB}(k',k)}{\omega_k + E_{B'} - W} a^\dagger(k')|\Psi_{B'}\rangle. \quad (1)$$

The first term represents the free meson (M) and the baryon (B), and defines the channel, the next term is a bare three-quark state, and the third term describes meson clouds around different isobars. Here, W is the invariant energy, J and I are the angular momentum and isospin of the meson–baryon system. The integration is taken in the principal value sense. The multi-channel K matrix can then be expressed as

$$K_{M'B'MB}(k, k') = -\pi \sqrt{\frac{\omega E_B}{k W}} \langle \Psi^{MB} | |V_{M'}(k')| | \Psi_{B'} \rangle, \quad (2)$$

where $V_{M'}(k')$ stands for the quark–meson vertex to be computed in the underlying quark model. Above the MB threshold, the meson amplitudes χ in (1) are proportional to the K matrix and are computed using the Lippmann–Schwinger equation. Finally, the scattering T matrix is obtained by solving the Heitler equation $T = K + iTK$.

The meson electro-production amplitudes can be calculated in the same framework by including the γN channel. Close to a resonance, the amplitude can be cast in the form

$$\mathcal{M}_{MB\gamma N}^{\text{res}} = \sqrt{\frac{\omega_\gamma E_N^\gamma}{\omega_\pi E_N}} \frac{\xi}{\pi \mathcal{V}_{NR}^\pi} \langle \widehat{\Psi}_{\mathcal{R}} | V_\gamma | \Psi_N \rangle T_{MB\pi N},$$

where the photon vertex V_γ acquires contributions from quarks and pions, ξ is the spin–isospin factor depending on the multipole, and the spin and isospin of the outgoing hadrons. Here $\langle \widehat{\Psi}_{\mathcal{R}} | V_\gamma | \Psi_N \rangle$ is the helicity amplitude; the resonance state $\widehat{\Psi}_{\mathcal{R}}$ is extracted from the residua in the second and the third term in (1) at the resonance pole.

4. The Roper resonance

As the underlying quark model we have taken the cloudy bag model, primarily because of its simplicity. In the first step, we considered only two inelastic channels, the $\pi\Delta$ channel, and — assuming that the two-pion decay proceeds mainly through the σ -meson — the σN channel. We have further assumed that the bare quark state in (1) is a mixture of the bare nucleon state and the bare Roper state in which one quark is excited to the $2s$ orbit: $\Phi_{\mathcal{R}} = \sin\theta(1s)^3 + \cos\theta(1s)^2(2s)^1$. Using only the three channels, we were able to reproduce the experimental behavior of the scattering amplitudes up to $W \sim 1600$ MeV; to reproduce the amplitudes at somewhat higher W , we included the second Roper resonance. In quark models, the πNR coupling constant turns out to be too weak to reproduce the large resonance width, mostly due to the orthogonality of the $1s$ and $2s$ orbits. In our approach, this coupling is strongly enhanced through the pion loops as well as through the mixing of the two bare configurations as shown in Fig. 2.

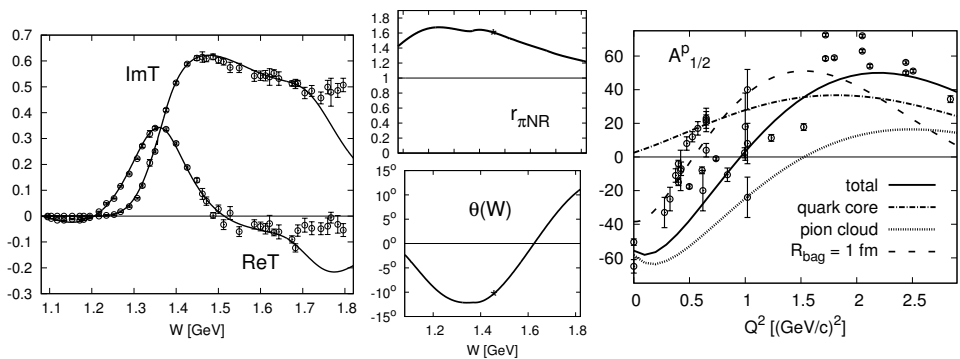


Fig. 2. The real and the imaginary part of the T-matrix in the P11 partial wave (left panel), the ratio of the dressed and the bare πNR coupling constants and the mixing angle θ as a function of W (middle panels), the quark and the pion contribution to the helicity amplitude $A_{1/2}^p$ in units of $10^{-3} \text{ GeV}^{-1/2}$ calculated in the cloudy bag model using the bag radius of 0.83 fm (right panel).

The role of the pion cloud is most strongly pronounced in the calculation of the helicity amplitude [4]. Here, the pion cloud plays an important role through the γNR vertex renormalization as well as through the direct coupling of the photon to the pion. In the region of low Q^2 , the quark contribution is small and positive, while the pion contribution and the vertex corrections due to meson loops are large and negative. At intermediate Q^2 , these two effects are responsible for the zero crossing of the amplitude. Using the bag radius of 1 fm instead of our standard choice of 0.83 fm, we are able to reproduce the popular value of $0.5 \text{ (GeV}/c)^2$ for the crossing point. At higher Q^2 , the quark core takes over, rendering the amplitude positive.

Let us mention that the sign of the helicity amplitude calculated in a model is ambiguous since the resonance production is a non-observable process. By convention, the sign is determined by the sign of the resonance decay within the same model. It is, therefore, not possible to compare different calculations of the helicity amplitudes if the sign of the decay amplitude is not provided.

5. The negative parity resonances

Here, the pion cloud consists predominantly of the s - and d -wave pions which are less strongly coupled to quarks than the p -wave pions in the case of positive parity resonances. Nonetheless, we have found some interesting phenomena that reveal the importance of the meson cloud also in this case.

In the S11 partial wave, there are two relatively close-lying resonances, the $N(1535)$ and $N(1650)$. In the quark model, these resonances appear as mixtures of two $\underline{70}$ -plet states with spin $1/2$ and $3/2$, *i.e.*: $|\Psi(1535)\rangle = \cos\theta|^2\mathbf{8}_{1/2}\rangle - \sin\theta|^4\mathbf{8}_{1/2}\rangle$ and $|\Psi(1650)\rangle = \sin\theta|^2\mathbf{8}_{1/2}\rangle + \cos\theta|^4\mathbf{8}_{1/2}\rangle$. It turns out that the mixing is such that only the lower state couples strongly to the ηN channel, while the coupling to this channel is almost absent for the higher state. In our calculation [5], we took a fixed angle of $\theta \approx 30^\circ$. A more elaborate calculation, including pion, η -meson and kaon loops shows that the mixing angle is generated entirely by the meson cloud effects and has a strong W dependence. As a consequence, it improves the behavior of the scattering amplitudes at smaller values of W (solid lines in Fig. 3) over the calculation with the fixed value of θ (dotted lines).

The pion cloud contribution to the helicity amplitudes is generally weak, of the order of 10%, except the case of the $\Delta(1700) 3/2^-$ resonance. Here we have found an almost equal contributions of the quark core and the pion cloud (see Fig. 4), quite a similar situation as in the case of its positive parity counterpart, the $\Delta(1232)$ [6].

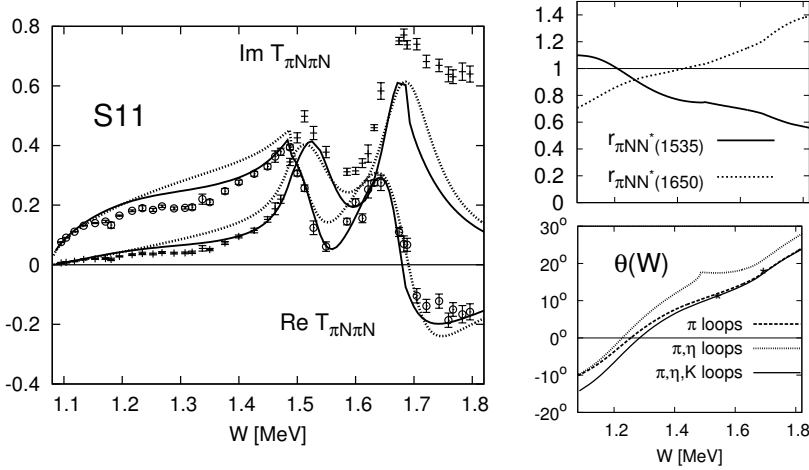


Fig. 3. The scattering T-matrix in the S11 partial wave (left panel), the renormalized πNN^* coupling constants for the two resonance and the mixing angle between the corresponding bare states as a function of W (middle panels).

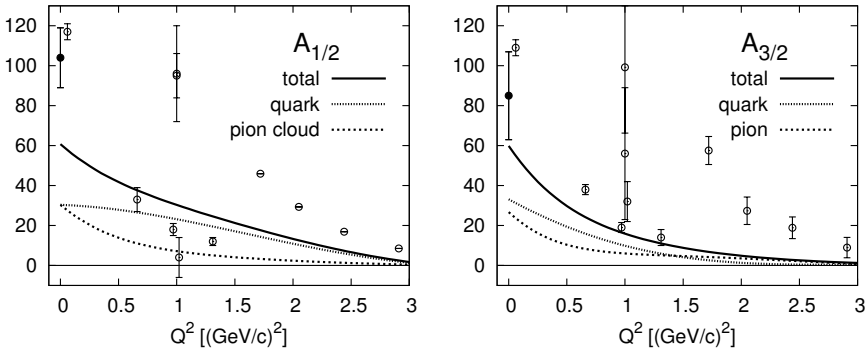


Fig. 4. The separate quark and pion contributions to the helicity amplitudes $A_{1/2}$ and $A_{3/2}$ for the $\Delta(1700)$ resonance.

The author would like to acknowledge the hospitality and the stimulating atmosphere he enjoyed during the workshop at the University of Coimbra.

REFERENCES

- [1] J. da Providência, J.N. Urbano, *Phys. Rev.* **D18**, 4208 (1978).
- [2] P. Alberto, M. Fiolhais, B. Golli, S. Širca, *Phys. Lett.* **B373**, 229 (1996).
- [3] B. Golli, S. Širca, *Eur. Phys. J.* **A38**, 271 (2008).
- [4] B. Golli, S. Širca, M. Fiolhais, *Eur. Phys. J.* **A42**, 185 (2009).
- [5] B. Golli, S. Širca, *Eur. Phys. J.* **A47**, 61 (2011).
- [6] B. Golli, S. Širca, *Eur. Phys. J.* **A49**, 111 (2013).